Methods to Crystallize RNA

Preparation of suitably large and well-ordered single crystals is usually the rate-limiting step in the determination of the three-dimensional structure of RNAs and their complexes with proteins by X-ray crystallography (reviewed by Holbrook and Kim, 1997). As illustrated by the examples of RNA and RNA-protein complexes in Table 7.6.1, successful crystallization conditions vary greatly for different molecules. A detailed protocol for the crystallization of even a limited set of RNAs cannot be written; therefore, we discuss a variety of experimental considerations relevant to obtaining RNA crystals for structure determination.

OVERVIEW

Biological macromolecules, as well as small molecules or simple salts, are crystallized from their metastable supersaturated solutions. When the system relaxes, some of the macromolecules come out of solution, yielding a solid phase which is in equilibrium with a saturated solution. Depending on the properties of the solvated molecule, and the conditions under which supersaturation and relaxation are achieved, the solid phase can consist of amorphous precipitate, a "shower" of microscopic crystals, or ideally, large single crystals. Successful growth of single crystals of macromolecules typically requires fine-tuning a large number of interdependent variables, and is thus often a formidable optimization problem.

The problem can be conquered by dividing it into a series of "unit operations" to be optimized in a recursive manner. First, a molecule or molecular complex must be designed or chosen to address the specific structural questions being posed and to have a good chance of being "crystallizable." Second, the molecule must be purified so that it is covalently homogeneous. Third, conditions must be found under which the molecule is conformationally homogeneous or monodisperse, and has full biochemical activity. Fourth, with a covalently and conformationally homogeneous sample in hand, a series of solution conditions in which the macromolecule might form supersaturated solutions can be screened. Fifth, if crystals result from these screens, they can be characterized and crystallization conditions further optimized. If crystals are not forthcoming, further optimization of preceding steps might be carried out. In the sections that follow, each of these steps is discussed.

CONSTRUCT DESIGN

The first consideration when crystallizing RNA is whether the molecule to be crystallized will be a short RNA (oligonucleotide) duplex, a non-duplex oligonucleotide, a larger RNA molecule, or an RNA-protein complex. Depending on the choice, the experimental strategies, as well as the likelihood of obtaining crystals of satisfactory quality with a given amount of effort, will vary. In general, oligonucleotide duplexes are the easiest to crystallize, and these crystals are most likely to be well ordered at the atomic level. Crystals of large RNAs are not necessarily difficult to obtain, but they are less likely to be well ordered. RNA-protein complexes fall somewhere in between in terms of their crystallizability and typical degree of order.

Oligonucleotide Duplexes

The double helix is the basic unit of RNA structure. Because of the strength of base-stacking interactions in aqueous solutions, crystals of short nucleic acid duplexes are typically dominated by pseudo-infinite stacks of helices that traverse the entire crystal. Side-by-side helical packing involves weaker interactions of backbone, and occasionally base, functional groups (Dickerson et al., 1994; Berman et al., 1996; Holbrook and Kim, 1997).

The strategy for the design of crystallizable oligonucleotides is based on these characteristics, and resembles the strategy for the crystallization of DNA-protein complexes (Aggarwal, 1990; Schultz et al., 1990). Duplexes are prepared that incorporate the RNA segment of biological or chemical interest and have additional base pairs on either or both ends to make their length consist of an integral number of helical turns, or some rational fraction thereof. The crystallographically allowed fractions are 1/2, 1/3, 1/4, and 1/6 (Burns and Glazer, 1990). In this way, formation of a pseudo-infinite helix with alignment of successive duplexes is promoted. The pitch of A- or B-form duplexes varies between 10 and 12 bp. The pitch of a crystallization candidate is unknown a priori; thus, the basic strategy for oligonucleotide crystallization is one of length variation.

Contributed by Adrian R. Ferré-D'Amaré and Jennifer A. Doudna

Biophysical Analysis of Nucleic Acids

Supplement 1

Table 7.6.1 Illustrative Examples of RNA and RNA-Protein Complex Crystals

Compound	Space group	Crystallization conditions	V_m (Å^3/Da)[a]	d_{min} (Å)[b]	Reference
"UUUG" RNA dodecamer (24 nt)	$P4_1$	30% PEG 4000; 0.2 M NH$_4$ acetate; 0.1 M citrate, pH 5.6; 8 mM spermine	2.9	2.6	Baeyens et al. (1995)
RNA "dodecamer" with Shine-Delgarno sequence (24 nt)	$P1$	30% MPDc; 400 mM MgCl$_2$; 40 mM cacodylate, pH 6.5; 32°C	2.0	2.8	Schindelin et al. (1995)
Loop E "dodecamer" (24 nt)	$C2$	5%-25% MPD; 5-25 mM MgCl$_2$; 50 mM cacodylate, pH 6.0; 20°C	2.8	1.5	Correll et al. (1997)
HIV-1 TAR, RNA fragment (27 nt)	$P1$	20% PEG 4000; 2.5 mM MgCl$_2$; 200 mM NH$_4$Cl; 100 mM CaCl$_2$; 50 mM cacodylate, pH 6.0; 19°C	2.2	1.3	Ippolito and Steitz (1998)
Pseudoknot (28 nt)	$P3_221$	18% sec-butanol; 5 mM MgCl$_2$; 2 mM spermidine; 100 mM MOPS, pH 7.0; 25°C	2.0	1.6	Su et al. 1999
Sarcin-ricin loop (29 nt)	$P6_122$	3.0-3.2 M (NH$_4$)$_2$SO$_4$; 20 mM MgCl$_2$; 50 mM MOPS, pH 7.0; 1 mM spermine; 2 mM CoCl$_2$; 20°C	2.7	2.1	Correll et al. (1998)
Hammerhead ribozyme-2′OMe inhibited (41 nt)	$P3_121$	23% PEG 6000; 10 mM Mg acetate; 100 mM NH$_4$ acetate; 1 mM spermine; 30 mM cacodylate, pH 6.5; 20°C	3.2	3.1	Scott et al. (1995a)
Hammerhead ribozyme-DNA inhibitor complex (47 nt)	$P3_221$	1.9-2.2 M (NH$_4$)$_2$SO$_4$; 0-100 mM MgCl$_2$; 0-2 mM spermine; 10 mM cacodylate, pH 6.0; 4°C	4.8	2.6	Pley et al. (1993)
5S rRNA fragment I (62 nt)	$P6_122$	1.35 M MgSO$_4$; 20 mM MES, pH 6.4; room temperature	3.2	3.0	Kim (1992); Correll et al. (1997)
Yeast tRNA^{Phe} (76 nt)	$P2_1$	10% dioxane; 5-15 mM MgCl$_2$; 1-2 mM spermine; 4°C	2.4	2.5	Ladner et al. (1972); Robertus et al. (1974)
Yeast tRNA^{Phe} (76 nt)	$P2_12_12_1$	10% iso-propanol or 10%-12% MPD; 10 mM MgCl$_2$; 1 mM spermine; 4°-6°C	3.0	2.3	Kim et al. (1971); Kim et al. (1974)
Yeast initiator tRNA (76 nt)	$P6_422$	2 M (NH$_4$)$_2$SO$_4$; 5 mM MgCl$_2$; 2 mM spermine	5.2	3.0	Schevitz et al. (1979); Basavappa and Sigler, (1991)
Tetrahymena group I intron P4-P6 domain (160 nt)	$P2_12_12_1$	17% MPD; 20 mM MgCl$_2$; 10 mM NaCl; 20 mM cacodylate, pH 6.0; 0.2 mM spermine; 10 M Co (III) hexammine; 30°C	3.4	2.5	Doudna et al. (1993); Cate et al. (1996)
Tetrahymena group I intron fragment (247 nt)	$P4_22_12$	19% MPD; 18 mM MgCl$_2$; 50 mM KCl; 0.5 mM spermine; 50 mM cacodylate, pH 6.0; room temperature	5.0	5.0	Golden et al. (1997)

Table 7.6.1 Continued

Compound	Space group	Crystallization conditions	V_m (Å³/Da)[a]	d_{min} (Å)[b]	Reference
Tetrahymena group I intron fragment (247 nt)	$P4_22_12$	19% MPD; 18 mM $MgCl_2$; 50 mM KCl; 0.5 mM spermine; 50 mM cacodylate, pH 6.0; room temperature	5.0	5.0	Golden et al. (1997)
U1A-RNA complex (21 nt + 11 kDa protein)	$P6_522$	1.8 M $(NH_4)_2SO_4$; 40 mM Tris·Cl, pH 7.0; 5 mM spermine; 20°C	3.2	1.7	Oubridge et al. (1994)
U2B″U2A′-RNA complex (24 nt + 31 kDa protein)	$P2_12_12$	1% PEG 600; 9 mM $MgCl_2$; 50 mM NaCl 0.25 mM spermine; 0.25% octyl glucoside; 50 mM Tris·Cl, pH 7.3	2.7	2.4	Price et al. (1998)
HDV ribozyme-U1A complex (72 nt + 11 kDa protein)	$R32$	14% PEG-MME 2000; 1 mM $MgCl_2$; 250 mM Li_2SO_4; 100 mM Tris·Cl, pH 7.0; 4.0 mM spermine; 0.2 mM Co (III) hexammine; 25°C	3.2	2.2	Ferré-DAmaré et al. (1998a)
Yeast AspRS-tRNA^{Asp} complex	$P2_12_12_1$	62% sat.$(NH_4)_2SO_4$; 5mM $MgCl_2$; 40 mM Tris·Cl, pH 7.5; 4°C	3.8	2.7	Ruff et al. (1988)
E. coli GlnRS-tRNA^{Gln} complex	$C222_1$	48% sat. $(NH_4)_2SO_4$; 20 mM $MgSO_4$; 80 mM PIPES, pH 7.4; 4 mM ATP; 17°C	3.7	2.5	Rould et al. (1991)

[a]V_m is the Matthews number (see text).
[b]d_{min} is the best reported diffraction.
[c]MPD is 2-methyl-2,4-pentanediol.

In a standard crystallization project, a series of duplexes are prepared that span the expected length of one (or several) helical turns. For instance, if the segment of interest is 8 bp, then oligonucleotides that range from 9 to 14 bp can be synthesized. The basic length screen should be augmented by varying the termini of the duplexes. Given the expectation that the duplexes will stack end-to-end, this variation is likely to have a strong influence on crystal growth and order. Overhanging ends, whose sequences might be complementary to those at the opposite end of the duplex, can be added to some of the duplexes, and the composition of the ends varied (if they are not part of the sequence whose structure is of interest). This can be achieved simultaneously with a length search by "mixing and matching" oligonucleotides of different lengths. The composition of the ends of oligonucleotides can have non-trivial effects because the stacking energies of different pairs of bases can vary by more than 10 kcal/mol (Saenger, 1984).

Table 7.6.1 includes four examples of oligonucleotide duplex crystals. The crystals of Baeyens et al. (1995), Schindelin et al. (1995), and Correll et al. (1997) are of duplex dodecamers which are almost exactly one helical turn in length. The HIV-1 trans-activation response region (TAR) fragment crystals of Ippolito and Steitz (1998) comprise a 15-nt strand with three bulged residues paired to a 12-nt strand. This effectively results in one complete turn of the atypical helix. The duplexes of Correll et al. (1997) and of Ippolito and Steitz (1998) incorporate 5′ overhangs. The other two are blunt-ended.

When designing asymmetric (nonpalindromic) oligonucleotides for crystallization, particular attention should be paid to possible undesired duplexes that the RNAs might form. If significant self-complementarity is present, a homoduplex might unexpectedly be favored over the desired heteroduplex, and crystals of an irrelevant duplex may result.

Limiting the lengths of duplexes to integral numbers of helix turns is favorable. The external surface of nucleic acid duplexes is dominated by the periodic negative charges of the phosphate backbone. In unlucky cases, du-

Biophysical Analysis of Nucleic Acids

7.6.3

plexes whose length is an irrational fraction of helical turns have produced beautiful, well diffracting crystals in which the helices stack head-to-tail in the crystal. On close inspection, some of these consist of infinite pseudo-continuous helices packed side-by-side, out of register with their sequence. If the structure can be solved, the electron density will consist of very well ordered sugar phosphate backbone (which produces the high-resolution diffraction) and poor base density which results from averaging the different bases which comprise the oligonucleotide. See Shah and Brunger (1999) for a detailed analysis of an example.

Complex Oligonucleotides

Under this heading we include short (~30 nt or less) RNAs whose biologically relevant structures are not simple duplexes, but have elements such as terminal loops or strand crossovers. These molecules usually comprise some sequences that are self-complementary, and a problem that often arises in crystallization is that the molecules disproportionate into duplexes, with the noncomplementary regions forming noncanonical base pairs.

For instance, crystallization of isolated stem-loops incorporating "tetraloop" sequences has often been hampered by the hairpin-loop to duplex equilibrium favoring of the duplex at the high RNA concentrations required for crystallization. The equilibrium probably favors the duplex because, in crystals, stacking occurs at both ends of the molecule, while the stem-loops only stack at one end (e.g., Holbrook et al., 1991). This can be exploited to study the structure of the noncanonical base pairs formed between the "loop" residues of the two strands (e.g., the "UUUG" RNA crystals of Baeyens et al., 1995; Table 7.6.1).

Despite this, some hairpin-loops have been crystallized. The 29-nt Sarcin-Ricin Loop crystals of Correll et al. (1998; Table 7.6.1) are stabilized by helix stacking at one end of the hairpin-loop, and by interactions between the loop nucleotides of adjoining molecules in the crystal. Similar interactions are observed in another case where a short stem-loop sequence was successfully crystallized (Perbandt et al., 1998). A 28-nt RNA which forms a classical pseudoknot (two helices stacked end-to-end, held by strand cross-overs in the major and minor grooves) has also been crystallized and its structure has been determined (Su et al., 1999; Table 7.6.1).

These successful examples suggest that a reasonable strategy for obtaining crystals of stem-loops might be to covalently constrain them from unpairing and duplexing. This might be achieved, for example, by introducing a disulfide bond linking the 5′ and 3′ termini (*UNIT 5.4*), or possibly by circularizing the RNA (Puttaraju and Been, 1992; *UNIT 5.2*). Stem-loops can also be stabilized by incorporating them into large RNA molecules.

Large RNAs

Large "globular" RNAs are composed of double-stranded helices, packed together to form substantial solvent-inaccessible cores (Ferré-D'Amaré and Doudna, 1999). In a manner similar to that with proteins, it is possible to define structural and functional domains in large RNAs. Often, these are better crystallization targets than the parent, multidomain molecules. Proteolysis is a powerful technique for defining the boundaries of protein domains (Cohen, 1996). Some RNA domains have been defined with the help of nucleases (e.g., 5S RNA fragment I; Kim, 1992; Correll et al., 1997; Table 7.6.1). Today, however, multiple sequence and secondary-structure alignments based on natural or artificial phylogenies constitute an expeditious means of searching for domain boundaries. Because the double helices that dominate RNA structure often bring together segments that are distant in primary sequence, secondary structures, based on sequence covariation and/or biochemical probing are, in general, the best starting point for domain-boundary elucidation for large RNAs.

The single-domain transfer RNAs were the first nucleic acids whose atomic structures were determined (Kim et al., 1974; Robertus et al., 1974). Other single-domain RNAs that have yielded crystal structures are the hammerhead ribozyme (Pley et al., 1994b; Scott et al., 1995b), Fragment I of the *E. coli* 5S rRNA (Correll et al., 1997), and a pseudoknot (Su et al., 1999; Table 7.6.1).

An extensive body of biochemical information has guided the design of crystallization constructs based on the Group I self-splicing intron of *Tetrahymena*. This large catalytic RNA can be divided into several structural domains which can be prepared separately, and when mixed, these will assemble to produce a functional RNA (Doudna and Cech, 1995). One of these, the 160-nt P4-P6 domain produced crystals that diffracted X-rays anisotropically to 2.5 and 2.8 Å (Doudna et al., 1993; Cate et al., 1996; Table 7.6.1). P4-P6 is an autonomously folding domain that is the first to acquire its structure in the kinetic folding pathway

of the intron, and nucleates folding of the complete RNA. Work on larger multidomain constructs of this class of catalytic RNAs has been partially successful (Doudna et al., 1993; Golden et al., 1997, 1998).

The design of crystallization constructs of the hammerhead ribozyme was also based on the biochemical knowledge of the system. Pley et al. (1993), and Scott et al. (1995a) varied the placement of the termini (and connectivity) of their molecules in the search for ribozymes that produced well-ordered crystals (Table 7.6.1). The crystallization of the hammerhead ribozymes also illustrates the use of different strategies for capturing one state of a catalytic molecule. While Pley et al. (1993) replaced the strand bearing the 2′- hydroxyl nucleophile with a DNA strand, Scott et al. (1995a) replaced the hydroxy group with a methoxy function. Both groups thus obtained structures of analogs of the ground-state of the catalytic RNA. As with proteins, binding of inhibitors and cofactors should be considered from the outset when crystallizing RNAs the interact with such molecules.

In designing crystallizable constructs of an RNA domain, or a multidomain RNA, length and end variation as practiced with oligonucleotide duplexes (Anderson et al., 1996) can be combined with other strategies, such as the circular permutation employed for the hammerhead ribozymes. In both crystal forms of the hammerhead, the blunt double-stranded ends of symmetry-related molecules stack on each other, and tetraloops placed at the distal ends of duplex stems also make various crystal contacts (Pley et al., 1994a; Scott et al., 1995b).

Crystallization of the same protein from several different species is a time-honored practice among crystallographers. Proteins from different sources often crystallize differently because the most phylogenetically variable residues in a folded macromolecule will lie on their surface. Surface residues are precisely those that will affect crystallization, as they will be responsible for crystal contacts and determine solubility. The same consideration applies to RNAs. Most of the variation in sequence between related RNAs occurs within duplex regions; some exposed variable residues will reside in helix terminal loops and can be varied to generate additional surface diversity (Golden et al., 1997).
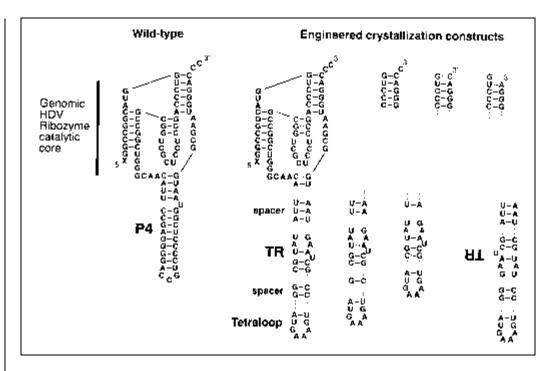
Surface variation can be taken one step further by incorporating crystallization modules into target RNAs (Ferré-D'Amaré et al., 1998b). These are moieties which are engineered into the sequence of the target RNAs in solvent-exposed portions so that they are available to make intermolecular interactions that can lead to crystal formation. One such crystallization module involves a GAAA tetraloop placed at the end of a duplex harboring its 11-nt receptor sequence. Since the two elements are stacked coaxially, they cannot dock intramolecularly, but can interact to pack neighboring molecules together. The module should be placed in a solvent-exposed portion of the target RNA, in a location that does not affect the activity (and by inference, the structure) of the parent molecule. In employing this technique, the placement of the crystallization module and the number of "spacer" nucleotides can both be varied (similar to the length variation for oligonucleotides) to generate a series of related RNAs that can be subjected to crystallization trials. Example RNA constructs based on this approach are shown in Figure 7.6.1.

RNA-Protein Complexes

Many biologically important RNAs carry out their functions in complexes with proteins. Crystals have been obtained both of complexes of unmodified full-length proteins and RNAs, and of engineered protein and RNA domains. Aminoacyl tRNA synthetase–tRNA complexes are examples of the former (e.g., Ruff et al., 1988; Rould et al., 1991; Table 7.6.1). In the two examples of an engineered complex in Table 7.6.1 (Oubridge et al., 1994; Price et al., 1998), both the proteins and the RNAs were optimized. Successful crystallization required careful definition of protein domain boundaries, mutational modification of the solvent-exposed surface of the protein, and a length search on the RNA moiety (Oubridge et al., 1995).

RNA-binding proteins can be employed as part of a second type of crystallization module. Crystals of a hepatitis delta virus (HDV) ribozyme which diffract X-rays to 2.2 Å were obtained by engineering the catalytic RNA so that its solvent-exposed, functionally dispensable stem-loop P4 was replaced by a high-affinity binding site for the U1A protein RNA-binding domain (Ferré-D'Amaré et al., 1998a; Table 7.6.1). The presence of the bound protein greatly facilitated crystallization, presumably because the RNA-protein complex has a larger variety of surface functional groups available for making crystal contacts than the naked RNA. In searching for good cocrystals, the authors made a series of constructs differing in the length of the spacer helix between the crystallization module and the catalytic core of the

Figure 7.6.1 Examples of constructs of a genomic hepatitis delta virus (HDV) ribozyme engineered for crystallization. The solvent-exposed P4 stem is dispensable for ribozyme function, and therefore unlikely to participate in the architecture of the catalytic core. Engineered crystallization constructs comprised a variety of substitute stem-loops incorporating a GAAA tetraloop, a tetraloop receptor (TR, in both orientations) and varying numbers of spacer base pairs (lower right). Additional variation was produced by progressive shortening of the 3′ terminus of the RNA (upper right). See text and Ferré-D'Amaré et al. (1998b) for details.

ribozyme, and also varied the termini of the ribozyme (Ferré-D'Amaré and Doudna, 2000). This strategy has been extended to other RNA targets.

Construct Design and the Phase Problem

Once well-ordered crystals have been produced, the phase problem must be overcome in order to obtain the three-dimensional structure. Thought should be given to heavy-atom derivative preparation when designing constructs. If the structure is to be solved either by the multiple isomorphous replacement (MIR) or multiwavelength anomalous diffraction (MAD) method, heavy atoms must be introduced to the RNA or RNA-protein complex. Traditionally, heavy atom derivatives were obtained by "soaking and praying," that is, by placing crystals in solutions of various heavy atom compounds at different concentrations, and then collecting X-ray data on the crystals to determine the effect of the soaks (Holbrook and Kim, 1985; Petsko, 1985). However, recombinant technology has made it possible to introduce heavy atoms covalently into the target molecules in advance of crystallization. For proteins and RNA-protein complexes, biosynthetic substitution of methionine with selenomethionine often provides excellent scatterers for MAD phasing (Doublié, 1997; Smith and Thompson, 1998). If an RNA or a segment of RNA is prepared by solid-phase synthesis, it is possible to substitute uracil with 5-bromouracil or cytosine with 5-bromocytosine (for instance, Correll et al., 1998; Ippolito and Steitz, 1998). Bromine is also an effective scatterer for MAD phasing. Synthetic introduction of phosphorothioates or thiols (which can later be bound to mercury or other heavy metals) into RNA is another possible approach. For large RNAs that bind tightly to either a small nucleic acid or a small molecule, heavy atom substitution of the ligand provides another means of obtaining a derivative. If a large RNA can be split into fragments without affecting biochemical activity and crystallizability, a small fragment could be prepared by chemical synthesis and modified to incorporate heavy atoms.

SAMPLE PREPARATION AND ANALYSIS

The vast majority of RNAs that are subjected to crystallization are prepared in vitro either by stepwise solid-phase chemical synthesis or by runoff transcription, using bacteriophage RNA polymerases. Some RNAs have been isolated from cells, and when post-transcriptional modifications are functionally and structurally important, this might be the method of choice. Synthesis and purification of RNA are covered in APPENDIX 3C.

Covalent homogeneity of starting materials is important for crystallization. In the case of synthetic RNA, substantial effort should be devoted to removing shorter impurities resulting from incomplete coupling. These can be removed either by preparative gel electrophoresis under denaturing conditions or by chromatographic methods. If phosphorothioates are being synthetically incorporated into the RNA, it might be desirable to resolve the diasteromers. Halogenated RNAs can be separated from molecules that have lost the halogen by anion-exchange chromatography at high pH by taking advantage of the perturbed pKa of N3 of bromouracil.

Runoff transcription with phage RNA polymerases results in molecules that are heterogeneous at their 3′, and sometimes their 5′ termini. In the case of shorter molecules, these impurities can be resolved by electrophoresis or chromatography. For larger RNAs (~40 nt or longer), these methods cease to work on a preparative scale. For these, *cis-* or *trans*-acting ribozymes can be employed to homogenize the termini (Price et al., 1995; Ferré-D'Amaré and Doudna, 1996). Another possibility is to cleave the transcripts using RNase H and a guide oligonucleotide (Lapham and Crothers, 1996).

If the crystallization target is a ribonucleoprotein complex, then attention should be paid to preparing a nuclease-free protein. Crystallization involves incubation of the protein-RNA complex for weeks to months and even a few contaminating nuclease molecules can hydrolyze large quantities of RNA in this time. The suitability of a protein preparation for cocrystallization with RNA should be evaluated by incubating the complex for a period of at least several days at room temperature.

Once purified, samples should be analyzed (i.e., electrophoresis, chromatography, or mass spectrometry), not only for covalent homogeneity, but also for conformational homogeneity. Since most RNAs are purified by denaturing methods, they often need to be refolded ("annealed"). This is usually accomplished by heating the RNA in the presence of divalent cations and buffer, then slowly cooling the solution to ambient temperature or lower. The success of a particular annealing protocol can be monitored by native gel electrophoresis, or physical methods such as dynamic light scattering (Ferré-D'Amaré and Doudna, 1997). In the case of larger RNAs with a well characterized biochemical activity, specific activity measurements provide a stringent indication of correct folding. For oligonucleotides, it is important to ascertain that the desired oligomerization state is the prevalent one, especially at high concentrations.

Conformational homogeneity of the macromolecular sample is often an excellent predictor of crystallizability (D'Arcy, 1994; Ferré-D'Amaré and Burley, 1997). If an RNA or RNA-protein complex is not monodisperse, annealing conditions can be further explored, ligands or inhibitors added, or the construct reengineered to increase homogeneity. Molecules that are polydisperse may crystallize. However, the amount of effort that must be expended to get crystalline material usually far exceeds that required to find a different construct that is monodisperse.

CRYSTALLIZATION TRIALS

Once pure, monodisperse, and fully biochemically active preparations are available in sufficient quantity, crystallization trials can begin. Depending on the solubility of the target molecule or complex, crystallization trials are carried out at concentrations of 1 to 20 mg/mL. There are a variety of experimental setups for screening crystallization conditions (reviewed in McPherson, 1990, 1999; Chayen et al., 1992; Ducruix and Geige, 1992; Weber, 1997). Of these, those favored by the authors are hanging-drop vapor diffusion and microbatch crystallization under oil for initial screens, because they require relatively small amounts of sample and can be set up quickly.

The most efficient way to search for crystallization conditions is by means of sparse matrix screens or incomplete factorial screens. Several such screens have been formulated. In the authors' laboratories, the screens of Doudna et al. (1993) and Scott et al. (1995a) are routinely employed for RNAs and the screen of Jancarik and Kim (1991), augmented with 1 mM spermine and varying concentrations of Mg^{2+}, is used for protein-RNA complexes. Other published screens include those of Carter and Carter (1979), Cudney et al. (1994), and Berger et

al. (1996). Because the goal of the crystallization setups is to achieve supersaturation, the concentration of the macromolecule is important. Generally, for initial screens, the authors consider it satisfactory when about one third of conditions produce precipitate within a few minutes of being mixed with the screen solution. If fewer conditions precipitate, the concentration of macromolecule should be raised, and vice versa.

As can be seen from Table 7.6.1, RNAs and RNA-protein complex crystals have been obtained from three broad classes of solutions: organic solvent-water mixtures, salt–polyethylene glycol (PEG) mixtures, and concentrated salt solutions. In screening for crystallization conditions for RNA, the authors have found that the sparse matrices of Scott et al. (1995a) and Doudna et al. (1993) complement each other well; the former is rich in salt/PEG mixtures, while the latter samples many organic solvents. Because of the polyanionic nature of RNA, all of the crystallization conditions include some cations, most often Mg^{2+} and spermine. Spermine has been employed for the overwhelming majority of successful RNA and RNA-protein complex crystallizations; it should initially be included in all screens.

Temperature has a profound effect on the crystallization behavior of macromolecules. At the very least, replicate screens should be set up at 4°C and room temperature (constant-temperature incubators at 20° to 25°C are preferable). Several RNAs crystallize better at temperatures higher than 30°C. Two examples in Table 7.6.1 are the Shine-Delgarno dodecamer of Schindelin et al. (1995) and the P4-P6 domain of Doudna et al. (1993). Replicate setups at 10° to 15°C and at 30°C are strongly recommended.

OPTIMIZATION OF CRYSTALLIZATION CONDITIONS

In the authors' experience, provided that construct design has been successful in producing monodisperse samples that have molecular surfaces favoring intermolecular interactions (such as the ends of oligonucleotide duplexes, or crystallization modules), at least some conditions in a crystallization screen should produce crystalline material within days to weeks. In extreme cases, crystals become visible upon minutes of setting up the screens.

Most crystals (except those in cubic space groups) are optically birefringent in some directions. Therefore crystallization trials are examined through a stereomicroscope under polarizers crossed so that the field is dark and birefringent objects show up brightly. If crystals have appeared, then the immediate goal is to characterize them to decide whether or not to thoroughly optimize the crystallization conditions. If the crystals are very small, some improvement of growth conditions might be needed before any characterization can be carried out.

The first question to be asked of any crystals is whether they are comprised of the RNA or RNA-protein complex of interest. If crystalline material is found in a vapor diffusion setup, one should immediately inspect the reservoir solution; if the setup was not airtight and has dried out, crystals might also be found in the reservoir. Macromolecular crystals are much more fragile than crystals of simple salts because they are typically comprised of 50% or more solvent by volume, being, in this sense, better described as oriented gels rather than crystals in the minerological sense. Therefore, if a crystal is poked with a scalpel or a thin wire and shatters easily, it is likely to be macromolecular. When sufficiently large crystals (~50 μm) become available, they should be washed free of mother liquor (which contains macromolecule in equilibrium with the crystal), dissolved, and analyzed by either electrophoretic, chromatographic, or mass spectrometric methods.

Crystals can usually be washed with the screen solution modified to contain an additional 10% to 30% of the precipitant, be it the organic solvent, PEG, salt, or polyamine. Before washing the crystals, as much mother liquor as possible should be removed; this should be analyzed as well to determine if there has been any nucleolytic or proteolytic degradation. The crystals should be washed by adding 5 to 10 μL of wash solution and pipetting it away. Washing can be repeated 2 to 3 times. The wash solutions should be analyzed as well, to ensure that the crystals were not dissolving during the process. Finally, the crystals can be dissolved in deionized water or dilute EDTA. Analysis of the resulting solution will demonstrate the composition of the crystals. A rough estimate of how much RNA or (RNA and protein) to expect to find in the last solution can be gained from calculating the volume of the crystal or crystals being dissolved (based on their exterior dimensions), and then assuming a typical solvent content (~60%) and a density of ~1 g/mL. If much less macromolecule than expected is found, and the crystals were not dissolving during the wash process, then the macromolecule in the last solution could be residual contamination from the mother liquor.

Crystallization consists of two distinct steps: nucleation and growth. In the first, thermodynamically unstable clusters of possibly as few as 100 molecules form. Once these nuclei grow beyond a certain point, growth becomes energetically favored (Stura and Wilson, 1990). Conditions under which nucleation and growth are favored are not necessarily the same, and can be experimentally separated. Seeding techniques are a powerful way to dissociate nucleation from growth, allowing conditions for both to be optimized separately. The techniques involved in protein crystal seeding have been reviewed elsewhere (Stura and Wilson, 1990) and apply to RNA and RNA-protein crystallization as well.

Optimization of crystallization conditions involves (1) determining what variables are relevant to nucleation and growth, and (2) what ranges and combination of ranges are optimal. The screen conditions under which crystals were obtained are the starting point for determining these parameters. Initially, it is important to sample broadly, because sparse matrices provide only a limited sampling of parameter space. For instance, if crystals grew in high concentrations of ammonium sulfate, follow-up screens should explore the effectiveness of lithium or magnesium sulfate in producing crystals. If crystals appear in conditions with PEG of average molecular weight 4000 (PEG 4000), then the effect of PEGs as well as PEG derivatives (e.g., polyethylene glycol monomethyl ethers; PEG-MMEs) of different average molecular weights should be explored. If these follow-up screens demonstrate that crystal growth is very sensitive to divalent cation concentration, then a variety of these, such as magnesium, manganese, calcium, barium, strontium, and cadmium, as well as metal hexammines, which mimic solvated magnesium, should be investigated. If calcium ions appear to be important for crystal formation, then lanthanides, which have similar coordination properties, should be tested. Temperature and pH should be varied in small steps to evaluate their effects on crystal growth.

Once the variables that are relevant to crystal formation have been determined, their optimal ranges and interactions must be investigated. This can be achieved by analytical techniques (i.e., response surface methods) such as those described by Carter (1997). However, the priority after discovering a new crystal form is not to find the optimal conditions for growth, but rather to obtain a few crystals which are large enough (~100 µm on the small dimension) to be placed in an X-ray beam to determine their degree of order. Because many RNA crystal forms do not diffract to high enough resolution to yield biochemical insights (see, for example, Ferré-D'Amaré et al., 1998b), too much effort should not be expended on a crystal form before it is known whether thorough optimization is warranted.

Ultimately, the most important property of crystals is how well they diffract X-rays. In order for a structure to yield biochemical insight, it is usually necessary to have X-ray data extending to at least 3.5 Å. A well refined structure at this resolution will have an average precision of atomic coordinates of the order of 0.3 to 0.5 Å, so that only the approximate location of atoms can be inferred from it. At a resolution of 2.0 Å, the coordinate error will typically be of the order of 0.1 to 0.2 Å, so that the presence of hydrogen bonds, for example, can be ascertained. At a resolution of 1.5 Å, details of hydration and coordination become apparent (Richardson and Richardson, 1985; Swanson, 1988). The highest resolution to which a crystal form will ultimately diffract, when large (~0.3 mm^3) specimens are exposed to very bright and well collimated X-rays from a synchrotron radiation source under cryogenic conditions, is difficult to estimate from initial diffraction measurements. If after several rounds of optimization the flash-cooled (see below) crystals fail to diffract beyond ~5 Å with a laboratory X-ray source with focusing mirrors, it is advisable to look for a different crystal form.

The analysis of X-ray diffraction data falls beyond the scope of this unit (see, for instance, Blundell and Johnson, 1976; Drenth, 1994). However, three pieces of information that result from a preliminary analysis are listed for different crystal forms in Table 7.6.1. These are the space group, or the symmetry rules that the crystals obey (Wukovitz and Yeates, 1995), the Matthews number (V_m), and the best diffraction (d_{min}). The space group (technically, the point group), the unit cell dimensions, the molecular weight of the macromolecule, and the number of molecules in the asymmetric unit (Z), yield the volume occupied per dalton of macromolecule, or V_m (Matthews, 1985). If the density of solvent is assumed to be that of water, then it can be shown (Matthews, 1968) that the volume fractions of the crystal occupied by macromolecule and solvent are:

$$V_{macromolecule} = 1.66\bar{v}/V_m$$

and

$$V_{solvent} = 1 - V_{macromolecule}$$

where $\bar{v}$ is the partial specific volume of the macromolecule. This is ~0.74 and 0.6 mL/g for proteins and RNA, respectively, so that for an RNA crystal, the solvent content is $\sim 1 - (1/V_m)$. Table 7.6.1 shows that V_m of RNA and RNA-protein complex crystals varies between 2.0 and 5.2. The best diffraction seen from a given crystal form correlates only loosely with solvent content (the regression coefficient for these 19 crystal forms is 0.62). Given the typical range of V_m, the number of molecules per asymmetric unit of a new crystal form can be guessed from the unit cell dimensions, the space group, and the molecular weight of the macromolecule. If the densities of the crystals and the crystallization solution are measured directly, then Z can be established rigorously (Matthews, 1985).

After measuring the first data set from a new crystal form, especially an oligonucleotide duplex, intensity statistics should be calculated to ascertain that the crystals do not suffer from twinning. See Yeates (1997) and Shah and Brunger (1999) for details.

Once a promising crystal form has been found from screens, a thorough optimization of growth conditions is warranted. In addition to a variety of possible additives (see above), seeding, analytical optimization methods, and modification of the crystallization setup should be attempted. For example, it is possible to change the crystallization kinetics of vapor diffusion setups by judicious use of oil (Chayen, 1997). Some crystal forms will grow better in a batch setup, or by microdialysis, rather than by vapor diffusion. The effects of varying the concentration of macromolecule and the kinetics of equilibration can be explored quickly in a diffusion setup by mixing different ratios of macromolecule stock and reservoir solutions when preparing the drops.

If analysis of the RNA (and if present, protein) in the crystal reveals nicking of the macromolecules, and the crystals show enrichment for a nicked species relative to mother liquor, it may be worthwhile to characterize the position of the nick. The shortened or nicked species may be a better crystallization construct. Furthermore, if there is enrichment in the crystals of some modified form of the macromolecule, then recrystallization may result in better ordered crystals.

Macromolecular crystals are damaged by exposure to X-radiation. This damage manifests itself as a decrease in intensity of the higher resolution reflections, and an increase in the mosaicity (Drenth, 1994) of the crystals.

Flash-cooling the crystals, so that the aqueous solutions surrounding the crystals and in the solvent channels of the crystals form an amorphous glass (Dubochet et al., 1988), permits data collection to be carried out at cryogenic temperatures (~100 K) which minimizes radiation damage. Most mother liquors will not form a glass when flash cooled; therefore, crystals must be transferred to a "cryoprotectant" solution. Optimization of the composition of this solution and the transfer protocol are important in obtaining the highest possible resolution diffraction from a given crystal form. This has been reviewed elsewhere (Rodgers, 1997; Harp et al., 1998). The authors' experience suggests that the cryoprotectants which have been successful for proteins and protein-DNA complexes will often work for RNAs and RNA-protein complexes.

CONCLUSION

Successful crystallization is an iterative optimization process. In this unit we have emphasized construct design, because in our experience this is the single most important factor in obtaining well-ordered RNA and RNA-protein complex crystals.

LITERATURE CITED

Aggarwal, A.K. 1990. Crystallization of DNA binding proteins with oligodeoxynucleotides. *Methods* 1:83-90.

Anderson, A.C., Earp, B.E., and Frederick, C.A. 1996. Sequence variation as a strategy for crystallizing RNA motifs. *J. Mol. Biol.* 259:696-703.

Baeyens, K.J., De Bondt, H.L., and Holbrook, S.R. 1995. Structure of an RNA double helix including uracil-uracil base pairs in an internal loop. *Nature Struct. Biol.* 2:56-62.

Basavappa, R. and Sigler, P.B. 1991. The 3 Å crystal structure of yeast initiator tRNA: Functional implications in initiator/elongator discrimination. *EMBO J.* 10:3105-3111.

Berger, I., Kang, C., Sinha, N., Wolters, M., and Rich, A. 1996. A highly efficient 24-condition matrix for the crystallization of nucleic acid fragments. *Acta Crystallogr. Sect. D Biol. Crystallogr.* 52:465-468.

Berman, H.M., Gelbin, A., and Westbrook, J. 1996. Nucleic acid crystallography: A view from the nucleic acid database. *Prog. Biophys. Mol. Biol.* 66:255-288.

Blundell, T.L. and Johnson, L.N. 1976. Protein Crystallography. Academic Press, London.

Burns, G. and Glazer, A.M. 1990. Space groups for solid state scientists. Academic Press, Boston.

Carter, C.W. 1997. Response surface methods for optimizing and improving reproducibility of crystal growth. *Methods Enzymol.* 276:74-99.

Carter C.W., Jr. and Carter, C.W. 1979. Protein crystallization using incomplete factorial experiments. *J. Biol. Chem.* 254:12219-12223.

Cate, J.H., Gooding, A.R., Podell, E., Zhou, K., Golden, B.L., Kundrot, C.E., Cech, T.R., and Doudna, J.A. 1996. Crystal structure of a group I ribozyme domain: Principles of RNA packing. *Science* 273:1678-1685.

Chayen, N.E. 1997. The role of oil in macromolecular crystallization. *Structure* 5:1269-1274.

Chayen, N., Stewart, P.D.S., and Blow, D.M. 1992. Microbatch crystallization under oil—a new technique allowing many small-volume crystallization trials. *J. Cryst. Growth* 122:176-80.

Cohen, S.L. 1996. Domain elucidation by mass spectrometry. *Structure* 4:1013-1016.

Correll, C.C., Freeborn, B., Moore, P.B., and Steitz, T.A. 1997. Metals, motifs, and recognition in the crystal structure of a 5S rRNA domain. *Cell* 91:705-712.

Correll, C.C., Munishkin, A., Chan, Y.-L., Ren, Z., Wool, I.G., and Steitz, T.A. 1998. Crystal structure of the ribosomal RNA domain essential for binding elongation factors. *Proc. Natl. Acad. Sci. U.S.A.* 95:13436-13441.

Cudney, B., Patel, S., Weisgraber, K., Newhouse, Y., and McPherson, A. 1994. Screening and optimization strategies for macromolecular crystal growth. *Acta Crystallogr. Sect. D Biol. Crystallogr.* 50:414-423.

D'Arcy, A. 1994. Crystallizing proteins—a rational approach? *Acta Crystallogr. Sect. D Biol. Crystallogr.* 50:469-471.

Dickerson, R.E., Goodsell, D.S., and Neidle, S. 1994. "... the tyranny of the lattice ...". *Proc. Natl. Acad. Sci. U.S.A.* 91:3579-3583.

Doublié, S. 1997. Preparation of selenomethionyl proteins for phase determination. *Methods Enzymol.* 276:523-530.

Doudna, J.A. and Cech, T.R. 1995. Self-assembly of a group I intron active site from its component tertiary structural domains. *RNA* 1:36-45.

Doudna, J., Grosshans, C., Gooding, A., and Kundrot, C.E. 1993. Crystallization of ribozymes and small RNA motifs by a sparse matrix approach. *Proc. Natl. Acad. Sci. U.S.A.* 90:7829-7833.

Drenth, J. 1994. Principles of Protein X-ray Crystallography. Springer-Verlag, New York.

Dubochet, J., Adrian, M., Chang, J.-J., Homo, J.-C., Lepault, J., McDowall, A.W., and Schultz, P. 1988. Cryo-electron microscopy of vitrified specimens. *Q. Rev. Biophys.* 21:129-228.

Ducruix, A. and Geigé, R. (eds.) 1992. Crystallization of Nucleic Acids and Proteins: A Practical Approach. Oxford University Press, Oxford.

Ferré-D'Amaré, A.R. and Burley, S.K. 1997. Dynamic light scattering in evaluating crystallizability of macromolecules. *Methods Enzymol.* 276:157-166.

Ferré-D'Amaré, A.R. and Doudna, J.A. 1996. Use of *cis*- and *trans*-ribozymes to remove 5′ and 3′ heterogeneities from milligrams of in vitro transcribed RNA. *Nucl. Acids Res.* 24:977-978.

Ferré-D'Amaré, A.R. and Doudna, J.A. 1997. Establishing suitability of RNA preparations for crystallization. Determination of polydispersity. *In* Ribozyme Protocols (P.C. Turner, ed.) pp. 371-378. Humana Press, Totowa, N.J.

Ferré-D'Amaré, A.R. and Doudna, J.A. 1999. RNA folds: Insights from recent crystal structures. *Annu. Rev. Biophys. Biomol. Struct.* 28:57-73.

Ferré-D'Amaré, A.R. and Doudna, J.A. 2000. Crystallization and structure determination of a hepatitis delta virus ribozyme: use of the RNA-binding protein U1A as a crystallization module. *J. Mol. Biol.* 295:541-556.

Ferré-D'Amaré, A.R., Zhou, K., and Doudna, J.A. 1998a. Crystal structure of a hepatitis delta virus ribozyme. *Nature* 395:567-574.

Ferré-D'Amaré, A.R., Zhou, K., and Doudna, J.A. 1998b. A general module for RNA crystallization. *J. Mol. Biol.* 279:621-631.

Golden, B.L., Podell, E.R., Gooding, A.R., and Cech, T.R. 1997. Crystals by design: A strategy for crystallization of a ribozyme derived from the Tetrahymena group I intron. *J. Mol. Biol.* 270:711-723.

Golden, B.L., Gooding, A.R., Podell, E.R., and Cech, T.R. 1998. A preorganized active site in the crystal structure of the Tetrahymena ribozyme. *Science* 282:259-264.

Harp, J.M., Timm, D.E., and Bunick, G.J. 1998. Macromolecular crystal annealing: Overcoming increased mosaicity associated with cryocrystallography. *Acta Cryatallogr. Sect. D Biol. Crystallogr.* 54:622-628.

Holbrook, S.R. and Kim, S.-H. 1985. Crystallization and heavy-atom derivatives of polynucleotides. *Methods Enzymol.* 114:167-176.

Holbrook, S.R. and Kim, S.-H. 1997. RNA crystallography. *Biopolymers* 44:3-21.

Holbrook, S.R., Cheong, C., Tinoco, I.J., and Kim, S.-H. 1991. Crystal structure of an RNA double helix incorporating a track of non-Watson-Crick base pairs. *Nature* 353:579-581.

Ippolito, J.A. and Steitz, T.A. 1998. A 1.3 Å resolution crystal structure of the HIV-1 trans-activation response region RNA stem reveals a metal ion-dependent bulge conformation. *Proc. Natl. Acad. Sci U.S.A.* 95:9819-9824.

Jancarik, J. and Kim, S.-H. 1991. Sparse matrix sampling: A screening method for crystallization of proteins. *J. Appl. Crystallogr.* 24:409-411.

Kim, J.L. 1992. X-ray crystallographic studies of a ribonuclease resistant fragment of *E. coli* 5S RNA. Ph.D. Dissertation, Yale University, New Haven, Conn.

Kim, S.-H., Quigley, G., Suddath, F.L., Rich, A. 1971. High-resolution X-ray diffraction patterns of crystalline transfer RNA that show helical regions. *Proc. Natl. Acad. Sci. U.S.A.* 68:841-845.

Biophysical Analysis of Nucleic Acids

7.6.11

Kim, S.-H., Suddath, F.L., Quigley, G.J., McPherson, A., Sussman, J.L., Wang, A.H.J., Seeman, N.C., and Rich, A. 1974. Three-dimensional tertiary structure of yeast phenylalanine transfer RNA. *Science* 185:435-440.

Ladner, J.E., Finch, J.T., Klug, A., and Clark, B.F.C. 1972. High-resolution X-ray diffraction studies on a pure species of transfer RNA. *J. Mol. Biol.* 72:99-101.

Lapham, J. and Crothers, D.M. 1996. RNase H cleavage for processing of in vitro transcribed RNA for NMR studies and RNA ligation. *RNA* 2:289-296.

Matthews, B.W. 1968. Solvent content of protein crystals. *J. Mol. Biol.* 33:491-497.

Matthews, B.W. 1985. Determination of protein molecular weight, hydration and packing from crystal densities. *Methods Enzymol.* 114:176-187.

McPherson, A. 1990. Current approaches to macromolecular crystallization. *Eur. J. Biochem.* 189:1-23.

McPherson, A. 1999. Crystallization of Biological Macromolecules. Cold Spring Harbor Press, Cold Spring Harbor, N.Y.

Oubridge, C., Ito, N., Evans, P.R., Teo, C.-H., and Nagai, K. 1994. Crystal structure at 1.92 Å resolution of the RNA-binding domain of the U1A spliceosomal protein complexed with an RNA hairpin. *Nature* 372:432-438.

Oubridge, C., Ito, N., Teo, C.-H., Fearnley, I., and Nagai, K. 1995. Crystallization of RNA-protein complexes II. The application of protein engineering for crystallization of the U1A protein-RNA complex. *J. Mol. Biol.* 249:409-423.

Perbandt, M., Nolte, A., Lorenz, S., Bald, R., Betzel, C., and Erdmann, V.A. 1998. Crystal structure of domain E of *Thermus flavus* 5S RNA: A helical RNA structure including a hairpin loop. *FEBS Lett.* 429:211-215.

Petsko, G.A. 1985. Preparation of isomorphous heavy atom derivatives. *Methods Enzymol.* 114:147-156.

Pley, H.W., Lindes, D.S., DeLuca-Flaherty, C., and McKay, D.B. 1993. Crystals of a hammerhead ribozyme. *J. Biol. Chem.* 268:19656-19658.

Pley, H.W., Flaherty, K.M., and McKay, D.B. 1994a. Model for an RNA tertiary interaction from the structure of an intermolecular complex between a GAAA tetraloop and an RNA helix. *Nature* 372:111-113.

Pley, H.W., Flaherty, K.M., and McKay, D.B. 1994b. Three-dimensional structure of a hammerhead ribozyme. *Nature* 372:68-74.

Price, S.R., Ito, N., Oubridge, C., Avis, J.M., and Nagai, K. 1995. Crystallization of RNA-protein complexes I. Methods for the large-scale preparation of RNA suitable for crystallographic studies. *J. Mol. Biol.* 249:398-408.

Price, S.R., Evans, P.R., and Nagai, K. 1998. Crystal structure of the spliceosomal U2B″U2A′ protein complex bound to a fragment of U2 small nuclear RNA. *Nature* 394:645-650.

Puttaraju, M. and Been, M.D. 1992. Group I permuted intron-exon (PIE) sequences self-splice to produce circular exons. *Nucl. Acids Res.* 20:5357-5364.

Richardson, J.S. and Richardson, D.C. 1985. Interpretation of electron density maps. *Methods Enzymol.* 115:189-206.

Robertus, J.D., Ladner, J.E., Finch, J.T., Rhodes, D., Brown, R.S., Clark, B.F.C., and Klug, A. 1974. Structure of yeast phenylalanine tRNA at 3Å resolution. *Nature* 250:546-551.

Rodgers, D.W. 1997. Practical cryocrystallography. *Methods Enzymol.* 276:183-203.

Rould, M.A., Perona, J.J., and Steitz, T.A. 1991. Structural basis of anticodon loop recognition by glutaminyl-tRNA synthetase. *Nature* 352:213-218.

Ruff, M., Mitschler, A., Cavarelli, J., Giegé, R., Mikol, V., Thierry, J.C., Lorber, B., and Moras, D. 1988. A high resolution diffracting crystal form of the complex between yeast tRNA^{Asp} and aspartyl-tRNA synthetase. *J. Mol. Biol.* 201:235-236.

Saenger, W. 1984. Principles of Nucleic Acid Structure. Springer-Verlag, New York.

Schevitz, R.W., Podjarny, A.D., Krishnamachari, N., Hughes, J.J., Sigler, P.B., and Sussman, J.L. 1979. Crystal structure of a eukaryotic initiator tRNA. *Nature* 278:188-190.

Schindelin, H., Zhang, M., Bald, R., Fürste, J.-P., Erdmann, V.A., and Heinemann, U. 1995. Crystal structure of an RNA dodecamer containing the *Escherichia coli* Shine-Delgarno sequence. *J. Mol. Biol.* 249:595-603.

Schultz, S.C., Shields, G.C., and Steitz, T.A. 1990. Crystallization of *Escherichia coli* catabolite gene activator protein with its DNA binding site the use of modular DNA. *J. Mol. Biol.* 213:159-166.

Scott, W.G., Finch, J.T., Grenfell, R., Fogg, J., Smith, T., Gait, M.J., and Klug, A. 1995a. Rapid crystallization of chemically synthesized hammerhead RNA's using a double screening procedure. *J. Mol. Biol.* 250:327-332.

Scott, W.G., Finch, J.T., and Klug, A. 1995b. The crystal structure of an all-RNA hammerhead ribozyme: A proposed mechanism for RNA catalytic cleavage. *Cell* 81:991-1002.

Shah, S.A. and Brunger, A.T. 1999. The 1.8 Å crystal structure of a statically disordered 17 base-pair RNA duplex: principles of RNA crystal packing and its effect on nucleic acid structure. *J. Mol. Biol.* 285:1577-88.

Smith, J.L. and Thompson, A. 1998. Reactivity of selenomethionine--dents in the magic bullet? *Structure* 6:815-819.

Stura, E.A. and Wilson, I.A. 1990. Analytical and production seeding techniques. *Methods* 1:38-49.

Su, L., Chen, L., Egli, M., Berger, J.M., and Rich, A. 1999. Minor groove RNA triplex in the crystal structure of a viral pseudoknot involved in ribosomal frameshifting. *Nature Struct. Biol.* 6:285-292.

Swanson, S.M. 1988. Effective resolution of macromolecular X-ray diffraction data. *Acta Crystallogr.* A44:437-442.

Weber, P.C. 1997. Overview of protein crystallization methods. *Methods Enzymol.* 276:13-22.

Wukovitz, S.W. and Yeates, T.O. 1995. Why protein crystals favor some space-groups over others. *Nature Struct. Biol.* 2:1062-1067.

Yeates, T.O. 1997. Detecting and overcoming crystal twinning. *Methods Enzymol.* 276:344-358.

Contributed by Adrian R. Ferré-D'Amaré
Fred Hutchinson Cancer Research Center
Seattle, Washington

Jennifer A. Doudna
Yale University
New Haven, Connecticut

Biophysical Analysis of Nucleic Acids

7.6.13